ELSEVIER

Size and Location of Ice Crystals in Pork Frozen by High-Pressure-Assisted Freezing as Compared to Classical Methods

M. N. Martino,[a]* L. Otero,[b] P. D. Sanz[b] & N. E. Zaritzky[a]

[a]Centro de Investigación y Desarrollo en Criotecnología de Alimentos (CIDCA), CONICET, Facultad de Cs. Exactas and Facultad de Ingeniería, Universidad Nacional de La Plata-Calle 47 y 116 (1900) La Plata, Argentina
[b]Instituto del Frío, CSIC-Ciudad Universitaria, Madrid, Spain

ABSTRACT

*In high-pressure-assisted freezing, samples are cooled under pressure (200 MPa) to −20°C without ice formation then pressure is released (0·1 MPa) and the high super-cooling reached (approx. 20°C), promotes uniform and rapid ice nucleation. The size and location of ice crystals in large meat pieces (*Longissimus dorsi *pork muscle) as a result of high-pressure-assisted freezing were compared to those obtained by air-blast and liquid* N_2*. Samples from the surface and centre of the frozen muscle were histologically analysed using an indirect technique (isothermal-freeze fixation). Air-blast and cryogenic fluid freezing, having thermal gradients, showed non-uniform ice crystal distributions. High-pressure-assisted frozen samples, both at the surface and at the central zones, showed similar, small-sized ice crystals. This technique is particularly useful for freezing large pieces of food when uniform ice crystal sizes are required. © 1998 Elsevier Science Ltd. All rights reserved*

INTRODUCTION

The advantages of food preservation by freezing (volatile retention, minimum change of organoleptic properties, absence of microbial growth, etc.) are to a certain extent counter-balanced by the damage caused by the formation of ice within the tissue. The size and location of ice crystals formed during freezing depend on the rate and final temperature of the process and affect important quality parameters like exudate, texture and colour of frozen products.

*To whom correspondence should be addressed. Fax: + 54 2124 9287; e-mail: mmartino@volta.ing.unlp.edu.ar

It is well known that the crystallisation of ice has two steps: the first is the formation of nuclei and the second is the later growth of the nuclei to a specific crystal size. Nucleation is an activated process whose driving force is supercooling (the difference between the actual temperature and that of the solid–liquid equilibrium). Greater supercooling achieves a larger number of generated nuclei. Nucleation also depends on the volume of the sample because of the statistical nature of nuclei formation. Ice crystal growth takes place after nucleation; water molecules add to the nuclei already formed, requiring only a minimum of subsequent supercooling (Fennema, 1973).

In frozen foods, the final size of ice crystals is a function of the rates of nucleation and crystal growth and also of final temperature. In slow freezing where the temperature of the sample remains close to the solid–liquid equilibrium curve for a long time, the rate of nucleation is low and only a few nuclei will be formed, leading to final large ice crystal sizes. On the other hand, in a system submitted to higher freezing rates, many nuclei will be formed, limiting the final crystal size.

In traditional freezing methods when a food product comes into contact with the refrigerating medium, ice nucleation occurs in the region next to the refrigerated border and is controlled by the magnitude of supercooling reached in this zone (Bevilacqua and Zaritzky, 1980). In the inner regions of the product, because of the thermal gradients, supercooling to produce ice nucleation is not acheived, resulting in the growth of large ice crystals.

The optimum freezing rate for food products or living cells is highly dependent on the system. Slow freezing generally results in extensive mechanical damage and decreases the maximum attainable food quality. Ultra-rapid freezing (e.g. cryogenic freezing), which leads to a food quality superior to that obtained by slow freezing, may cause lethal intracellular ice crystallisation in living cells or mechanical cracking (Kalichevsky *et al.*, 1995). At atmospheric pressure, water which freezes has a volume increase of approximately 9%, characteristic of ice I with its unique property of a lower density than liquid water (Kalichevsky *et al.*, 1995). Cryogenic freezing often induces cracking, particularly in large samples with high water content and low porosity (Kim and Hung, 1994). This may be owing to a non-uniform contraction following solidification or the rupture of the outer frozen shell when the interior region freezes and expands or a combination of both of these mechanisms (Love, 1966; Fennema, 1973).

The main applications of pressure in relation to the water-phase diagram are the high freezing rates obtained using pressure-assisted freezing, cryoinmobilisation to analyse the ultrastructure of biological specimens at glassy state, high thawing rates and non-frozen storage at subzero temperatures (Deuchi and Hayashi, 1992; Kanda *et al.*, 1992; Studer *et al.*, 1992; Lüdemann, 1994; Kalichevsky *et al.*, 1995; Fuchigami *et al.*, 1996). High pressure reduces the melting point of water to a minimum at about $-21°C$ at 210 MPa, the triple point for liquid water–ice I–ice III (Fig. 1), thus, as long as the specimen is above this point, water remains unfrozen. The present work focuses on high-pressure-assisted freezing where samples are cooled under pressure (200 MPa) to $-20°C$ without ice formation then pressure is released to atmospheric pressure, obtaining a high supercooling. An insight into the microstructure of food processed by this technique becomes necessary to explore potential food applications. Nowadays, the biggest obstacle to high-pressure processing is cost, mainly capital costs because operating costs are not excessive and the technology is environmentally friendly (Mertens and Deplace, 1993; Ledward, 1995). Japan has the first example of implementing high-pressure processes commercially, and the USA and European industries are exploring this possibility as well (Cheftel, 1991; Knorr, 1993; Demetrakakes, 1996; Mermelstein, 1997).

The objective of this work was to analyse the size and location of ice crystals formed in pork meat frozen by high-pressure-assisted freezing as compared to industrial freezing methods such as liquid N_2 and air-blast freezing.
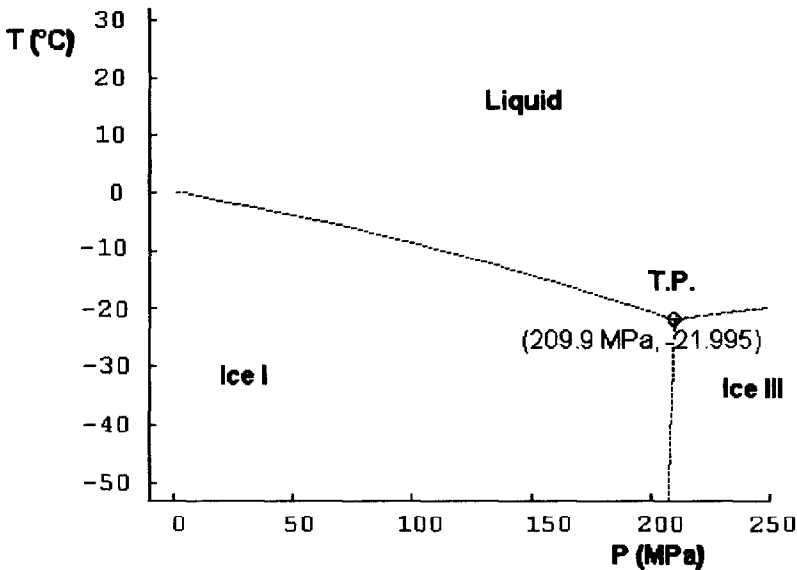
Fig. 1. Equilibrium solid–liquid phase diagram of water.

MATERIALS AND METHODS

Pieces of *longissimus dorsi* post-rigor pork muscles of about $5 \times 7.5 \times 11 \, cm^3$ were cut with the principal axis parallel to the muscle fibres. These dimensions were chosen to allow the observation of thermal gradients. Each sample was packed in a polyethylene bag and two thermocouples of copper-constantan were inserted in the samples: one at the surface and the other at the centre.

High-pressure-assisted freezing was carried out in an experimental device (ACB GEC ALSTHON, Nantes, France) located at the Instituto del Frío, Madrid, Spain, equipped with a thermally isolated thermostatic circuit and with a pressure and temperature computerised measurement system (Fig. 2). The unit had a $2.35 \, dm^3$ free volume vessel and was operated at 200 MPa and $-20°C$ with ethyleneglycol–water as immersion fluid. The temperature of the immersion fluid was recorded by thermocouples located at the inlet and outlet of the thermostatic fluid circuit (Sanz *et al.*, 1997).

Two classical methods: air-blast freezing (representing a method with a low freezing rate) and liquid N_2 freezing (a very rapid freezing method) were compared with high-pressure-assisted freezing. Air-blast freezing (FRIGOSCANDIA SA, Paris, France) was carried out at $-35°C$ and an air speed of about $5.5 \, m/s$. Liquid N_2 freezing was performed in an experimental device consisting of an isolated box containing a grid where the sample remained during freezing. For both methods, the freezing process finished when the temperature at the centre of the sample was $-20°C$; then the electrical power in the air-blast freezer was switched off as well as the liquid N_2 supply in the cryogenic freezing process. In all cases thermal histories were recorded by copper-constantan thermocouples located at the border and the centre of the samples.

For the three freezing methods, experiments were performed at least in duplicate. Immediately after freezing, meat pieces were placed in a chamber at $-20°C$. Inside this chamber, small cylindrical samples of about 5 mm in diameter and 5 mm in height were taken for histological analysis. Four samples were taken from each piece of meat; two of them located at the surface and the others at the centre. The samples were placed in small
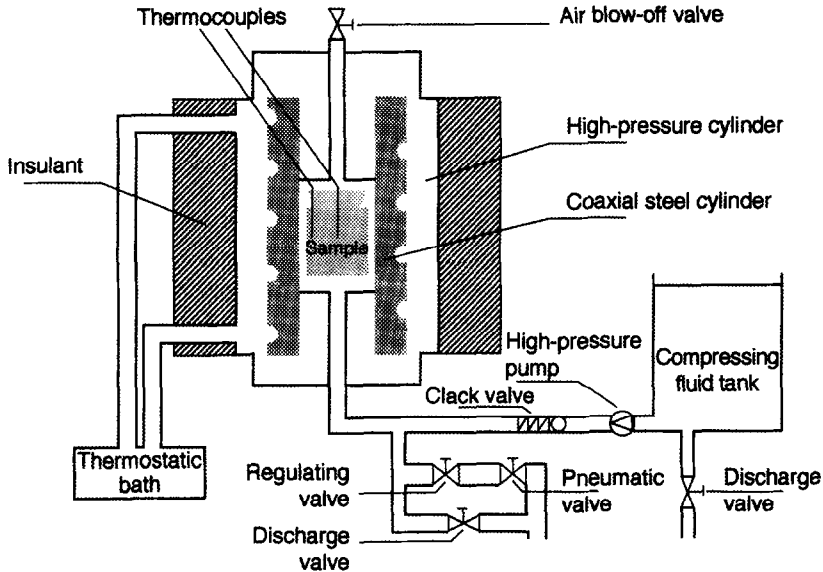
Fig. 2. Diagram of high-pressure freezing device.

flasks containing a fixative solution at −20°C. For microscopy analysis, an indirect technique was used based on observations of the holes left by the ice in the tissue. According to the isothermal freeze substitution technique, samples were fixed at the final freezing temperature (−20°C) with Carnoy fluid (60% absolute ethanol, 30% chloroform and 10% glacial acetic acid, v/v), which has a low freezing point and diffuses rapidly through the tissue (Martino and Zaritzky, 1986). Once fixed, samples were brought to room temperature, dehydrated with a series of ethanol solutions of gradually increasing concentrations, cleared in benzene and embedded in paraffin. Samples were cut with a rotary microtome (American Optical, Model 820, USA) in 15 μm thick sections. Sections were stained with haematoxylin-eosin and observed with a Leitz Ortholux II microscope equipped with a Leitz Vario Orthomat camera (Leitz, Germany). Unfrozen samples were used as controls; some of them at atmospheric pressure and the others submitted to 210 MPa.

Micrographs were digitised; the holes left by the ice were counted and their equivalent diameters were measured. Equivalent diameter was defined as the diameter of the circle that had the same area as the studied ice crystal. Mean crystal diameters and standard deviations were obtained from more than 100 measured holes.

RESULTS AND DISCUSSION

Temperature and pressure variations recorded during the high-pressure-assisted freezing process are shown in Fig. 3. The process began when unfrozen meat was placed in the high-pressure chamber (point A) and compressed up to 210 MPa (point B). The sample was then cooled without freezing to −20°C (point C), which was close to the liquid–ice I equilibrium curve (about −21°C and 210 MPa, Fig. 1). After a uniform temperature of −20°C was reached, an expansion to atmospheric pressure took place (point C to D). At point D, the temperature corresponds to a supercooling of about 20°C and, consequently, a massive nucleation occurred. Sample temperature increased to its melting temperature
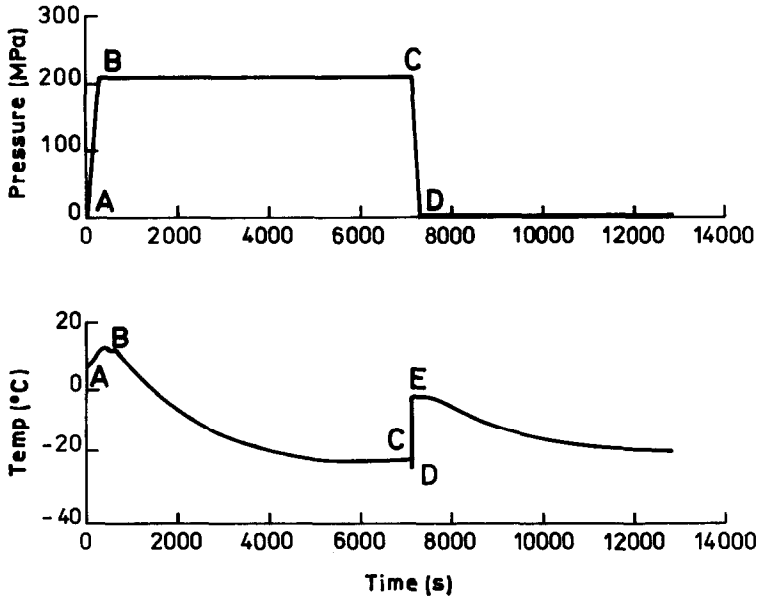
Fig. 3. Typical thermal and pressure histories of samples processed by high-pressure assisted freezing. A–B, compression; B–C, cooling at constant pressure; C–D, expansion to atmospheric pressure; E, melting point of ice I at atmospheric pressure.

at atmospheric pressure (−1·1°C, point E) because of the latent heat release. In high-pressure-assisted freezing, crystal growth, after nucleation, proceeds similarly to classical freezing at atmospheric pressure.

Micrographs of unfrozen pork tissue at atmospheric pressure [Fig. 4(a)] and submitted to 210 MPa [Fig. 4(b)] suggest that pressure, by itself, did not induce fibre distortion. Figures 5(a) and (b) show samples frozen by high-pressure-assisted freezing, corresponding to the surface and central zones, respectively. Samples located at the centre of the meat piece [Fig. 5(b)] showed small ice crystals whose distribution is comparable to that of samples located at the surface of the piece [Fig. 5(a)]. The small ice crystals located inside and outside the cells had a maximum equivalent diameter of about 7 μm at the intracellular space. Table 1 shows mean ice crystal diameters at the surface and central zones of the meat piece. These results can be attributed to the high and uniform supercooling (about 20°C) produced in the meat piece during the expansion step. According to Burke and co-workers (Burke *et al.*, 1975), for each °C of supercooling there is an increase of about tenfold in the ice nucleation rate, thus in our case a 200-fold increase in nucleation could have occurred. In previous work, Sanz *et al.* (1997) showed that about 36% of total water could be instantaneously converted to ice during the expansion, thus producing a massive nucleation with a large number of small crystals. The location of ice crystals in the tissue is a function of freezing rate, specimen temperature and the nature of the cells (Fennema, 1973). It is generally accepted that ice nucleation begins in extracellular regions, but, when the heat removal rate is high enough to eliminate more heat from the system than that originated by the crystallisation of extracellular ice, intracellular crystallisation can also take place within the fibres. These concepts can be applied to our work, where even in the central zones the ice crystal pattern corresponds to a high freezing rate.

(a)
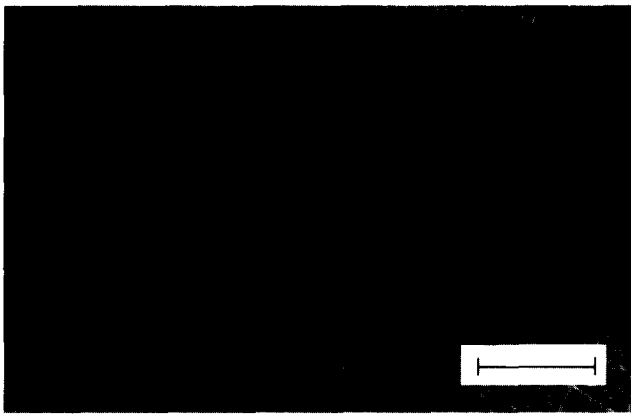
(b)

Fig. 4. Micrographs of unfrozen *longissimus dorsi* pork tissue (a) at atmospheric pressure and (b) processed at 210 MPa. Scale bar: 50 μm.

TABLE 1

Mean Ice Crystal Diameters (D, in μm) and Confidence Limits at the Surface and Centre of Samples Frozen by Different Methods

Freezing method	Surface	Centre
High-pressure-assisted freezing	2·34 ± 1·08	4·13 ± 2·46
Liquid N₂ freezing	3·03 ± 1·76	18·81 ± 1·36
Air-blast freezing	20·10 ± 3·04	31·11 ± 7·24

Traditional freezing of meat cuts involves important temperature gradients, which lead to a distribution of local freezing rates along the food piece. The higher freezing rates are reached at the border of the sample and decrease towards the centre. The local freezing rates can be quantified in terms of the characteristic freezing time (Bevilacqua *et al.*, 1979), defined as the time taken by the analysed sample point to pass from $-1°C$ (beginning of freezing) to $-7°C$ (freezing of 80% of the water present in meat tissue).
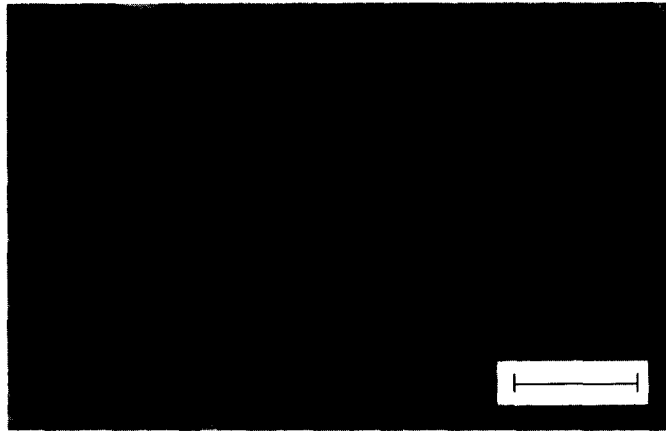
(a)
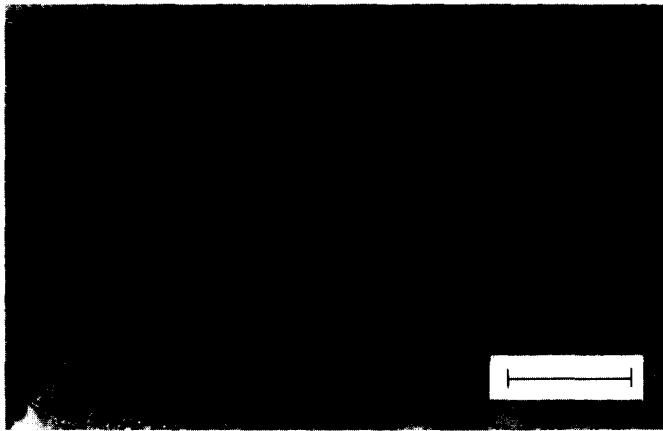
(b)

Fig. 5. Micrographs of *longissimus dorsi* pork tissue frozen by high-pressure-assisted freezing: (a) the surface zone and (b) the central zone. Scale bar: 50 μm.

The effect of the thermal gradient on microstructure is evidenced by the micrographs of meat frozen by liquid N_2 corresponding to the surface, semi-radius position and central zone of the meat piece, shown in Fig. 6 (a–c), respectively. The characteristic freezing time for the border of the sample was 7 min and for the centre was 21 min. The maximum ice crystal diameter in the intracellular space of samples located at the surface of the meat piece was about 8 μm. At the centre of the product, the average ice crystal diameter was much higher than that at the surface (Table 1). During cryogenic freezing, the system is able to remove enough heat to produce nucleation inside the fibres and with these high freezing rates water remains within the cells. However, because of the thermal gradients, this is only possible at the surface of the product. The more external region, near the refrigerated border [Fig. 6(a)], shows intra- and extracellular ice, the extracellular ice with only a small fraction of the tissue volume. The conditions that produce intracellular crystallisation give origin to many small ice crystals, a minimal dislocation of water and an aspect similar to unfrozen tissue. However, the internal zone of the sample shows larger
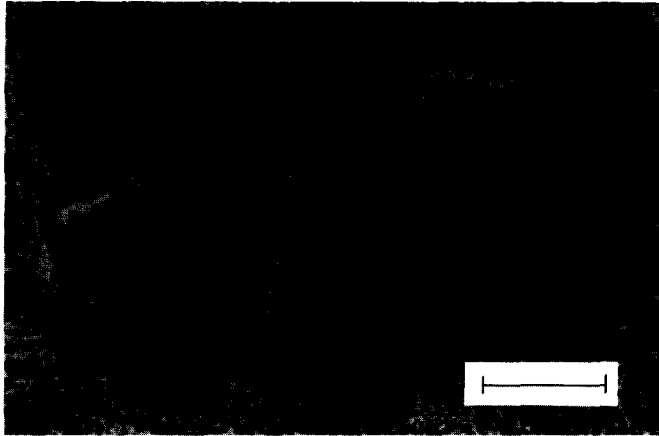
(a)
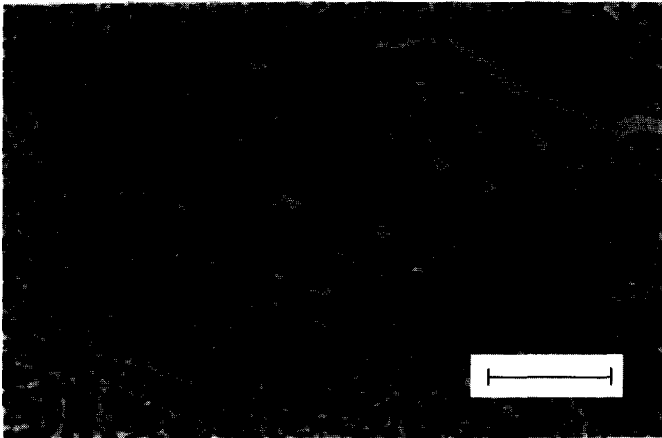
(b)
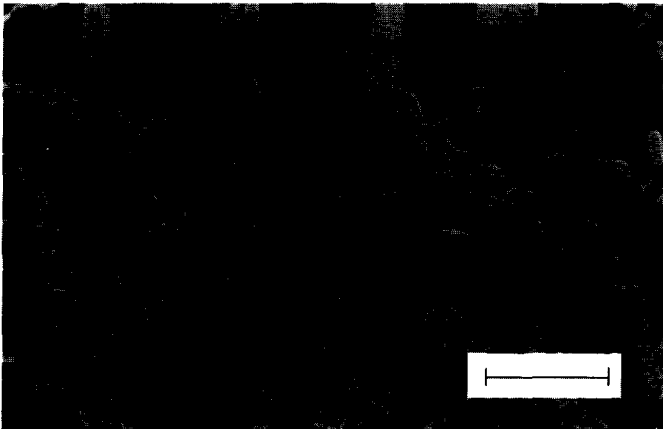
(c)

Fig. 6. Micrographs of *longissimus dorsi* pork tissue frozen by liquid N_2: (a) the surface zone, (b) the semi-radius position and (c) the central zone. Scale bar: 50 μm.

intra- and extracellular ice crystals that distort the original fibre matrix [Fig. 6(c)]. Thus, from the microstructural point of view, when working with large food pieces, the benefits attributed to cryogenic freezing are limited to the external zone (Otero *et al.*, 1997).

When meat was frozen by air-blast (low freezing rate), only extracellular ice crystals appeared [Fig. 7(a) and (b)]. During slow freezing, as ice forms in the extracellular regions, the solute concentration of the unfrozen phase gradually increases, thus decreasing the vapor pressure. Since crystals apparently cannot penetrate cellular membranes at relatively high subfreezing temperatures, the intracellular fluid remains supercooled, and its vapor pressure exceeds that of the extracellular fluid and ice crystals. Cellular dehydration takes place since water diffuses from the cells because of the vapor pressure difference. Water deposits on extracellular ice crystals. Intracellular supercooling decreases, together with intracellular nucleation probability. Thus, slow freezing results in considerable shrinkage of the cells and formation of large, exclusively extracellular, ice crystals (Love, 1966; Meryman, 1966; Fennema, 1973). Mean ice crystal diameters measured on the
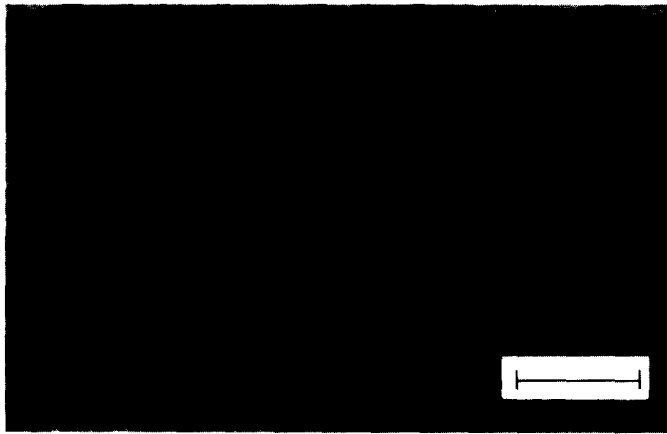
(a)

(b)

Fig. 7. Micrographs of *longissimus dorsi* pork tissue frozen by air-blast: (a) the surface zone and (b) the central zone. Scale bar: 50 μm.

micrographs corresponding to the surface and central zones are shown in Table 1. The characteristic freezing times were 24 min for the surface zone and 62 min for the central zone. These data compare well with those of Bevilacqua and co-workers (1979) and Bevilacqua and Zaritzky (1980) who measured ice crystal diameters in beef tissue frozen over a wide range of freezing conditions.

In large meat pieces, after nucleation near the refrigerated border, melting temperature is soon reached because of the release of latent heat, and no more nuclei can be formed. Then, freezing of the remaining water is produced by the subsequent heat removal (mainly by conduction) through frozen tissue. Thus, the few nuclei formed in the system grow to very big ice crystals from the surface of the product to the centre at the expense of the water released by the fibres. Compared to unfrozen control samples [Fig. 4(a)], these large crystals lead to fibres that are partially dehydrated and distorted.

According to Calvelo (1981), for the usual air-blast freezing of beef the zone with intracellular crystals is very small, about 1–2 cm from the refrigerated border, therefore a substantial part of industrially frozen cuts is characterised by extracellular and partially dehydrated, irregularly shaped fibres. For liquid N_2 freezing, the damage in cell structure at the surface zone is minimal; however, at the centre, it is similar to that produced in air-blast freezing. As can be observed, two of the most common problems that appear in classical freezing methods are low freezing rates and thermal gradients. Similar results were obtained by Kanda *et al.* (1992) and Fuchigami *et al.* (1996) working on tofu and carrots, respectively. They stressed that pressure-shift freezing between 200 MPa and 400 MPa and below −20°C maintained better product microstructure than other freezing methods.

In conclusion, the main advantage of high-pressure-assisted freezing is that ice nucleation occurs instantaneously and uniformly along the whole volume of the sample because of the high supercooling reached when the expansion takes place. From the microstructural point of view, the damage produced to the cells is minimal because of the small size of the ice crystals. This freezing method can therefore be especially useful for freezing foods with large dimensions in which a uniform ice crystal distribution is required and where important thermal gradients would be observed when applying classical freezing methods, including cryogenic freezing.

ACKNOWLEDGEMENTS

REFERENCES

Bevilacqua, A. E. and Zaritzky, N. E. (1980) Ice morphology in frozen beef. *Journal of Food Technology* **15**, 589–597.

Bevilacqua, A. E., Zaritzky, N. E. and Calvelo, A. (1979) Histological measurements of ice in frozen beef. *Journal of Food Technology* **14**, 237–251.

Burke, M. J., George, M. F. and Bryant, R. G. (1975) In *Water Relations of Foods*, ed. R. B., Duckworth, p. 111. Academic Press, London.

Calvelo, A. (1981) In *Developments in Meat Science, 2*, ed. R. Lawrie, p. 125. Applied Science Publishing, London.

Cheftel, J. C. (1991) Applications des hautes pressions en technology alimentaire. *Actualité des Industries Alimentaire et Agro-Alimentaires* **108**(3), 141–153.

Demetrakakes, P. (1996) The pressure is on. *Food Processing* February, 79–80.

Deuchi, T. and Hayashi, R. (1992) High pressure treatments at subzero temperature: application to preservation, rapid freezing and rapid thawing of foods. In *High Pressure and Biotechnology*, eds C. Balny, R. Hayashi, K. Heremans and P. Masson, Vol. 224, pp. 353–355. Colloque INSERM, John Libbey Eurotext Ltd, Montrouge, France.

Fennema, O. R. (1973) Nature of freezing process. In *Low Temperature Preservation of Foods and Living Matter,* eds O. R. Fennema, W. D. Powrie, and E. H. Marth, pp. 151–222. Marcel Dekker, New York.

Fuchigami, M., Kato, K. and Teramoto, A. (1996) Effect of pressure-shift freezing on texture, pectic composition and histological structure of carrots. In *High Pressure Bioscence and Biotechnology*, eds R. Hayashi and C. Balny, pp. 411–414. Elsevier, Amsterdam.

Kalichevsky, M. T., Knorr, D. and Lillford, P. J. (1995) Potencial food applications of high-pressure effects on ice-water transitions. *Trends in Food Science and Technology* **6**(8), 253–258.

Kanda, Y., Aoki, M. and Kosugi, T. (1992) Freezing of tofu by pressure freezing and its structure. *Nippon Shokuhin Kogyo Gakkaishai* **39**(7), 608–614.

Kim, N. K. and Hung, Y. C. (1994) Freeze-cracking in foods as affected by physical properties. *Journal of Food Science* **59**(3), 669–674.

Knorr, D. (1993) Effects of high-hydrostatic-pressure processes on food safety and quality. *Food Technology* **47**(6), 156, 158–161.

Ledward, D. A. (1995) High-pressure processing. The potential. In *High Pressure Processing of Foods*, eds. D. A. Ledward, D. E. Johnston, R. G. Earnshaw, and A. P. M. Hasting, pp. 1–5. Nottingham University Press, Loughborough, UK.

Love, R. M. (1966) The freezing of animal tissue. In *Cryobiology*, ed. H. Meryman, pp. 317–405. Academic Press, London.

Lüdemann, H. D. (1994) Water and its solutions at high pressures and low temperatures. *Polish Journal of Chemistry* **68**, 1–22.

Martino, M. N. and Zaritzky, N. E. (1986) Fixing conditions in the freeze substitution technique for light microscopy observation of frozen beef tissue. *Food Microstructure* **5**, 19–24.

Mermelstein, N. H. (1997) High-pressure processing reaches the US market. *Food Technology* **51**(6), 95–96.

Mertens, B. and Deplace, G. (1993) Engineering aspects of high-pressure technology in the food industry. *Food Technology* **47**(6), 164–169.

Meryman, H. (1966) Review of biological freezing. In *Cryobiology*, ed. H. Meryman, pp. 2–114. Academic Press, London.

Otero, L., Martino, M. N., Sanz, P. D. and Zaritzky, N. E. (1997) Histologic analysis of ice crystals in pork frozen by liquid N_2 and high-pressure-assisted freezing. *Scanning* **19**(3), 241–242.

Sanz, P. D., Otero, L., de Elvira, L. and Carrasco, J. A. (1997) Freezing processes in high-pressure domains. *International Journal of Refrigeration* **20**(5), 301–307.

Studer, D., Hennecke, H. and Müller, M. (1992) High-pressure freezing of soybean nodules leads to an improved preservation of ultrastructure. *Planta* **188**, 155–163.